AD-A046 697   AEROSPACE CORP   EL SEGUNDO CALIF IVAN A GETTING LABS   F/G 9/1
             MEASURED AND PREDICTED RADIATION-INDUCED CURRENTS IN SEMIRIGID --ETC(U)
             OCT 77 F HAI, P A BEEMER, C E WULLER   F04701-77-C-0078
UNCLASSIFIED   TR-0078(3950-04)-1   SAMSO-TR-77-203   NL

1 OF 1
ADA
046697

END
DATE
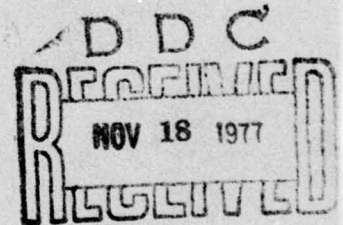FILMED

12-77
DDC

ADA046697

Measured and Predicted Radiation-Induced Currents in Semirigid Coaxial Cables

Materials Sciences Laboratory
The Ivan A. Getting Laboratories
The Aerospace Corporation
El Segundo, Calif. 90245
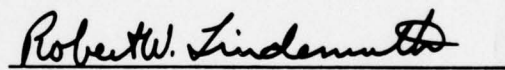
11 October 1977

Interim Report
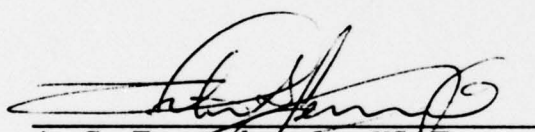
DDC
NOV 18 1977
A

AD No.
DDC FILE COPY

This interim report was submitted by The Aerospace Corporation, El Segundo, CA 90245, under Contract No. F04701-77-C-0078 with the Space and Missile Systems Organization, Deputy for Advanced Space Programs, P. O. Box 92960, Worldway Postal Center, Los Angeles, CA 90009. It was reviewed and approved for The Aerospace Corporation by W. C. Riley, Director, Materials Sciences Laboratory. Lt. A. G. Fernandez, SAMSO/YCPT, was the project officer for Advanced Space Programs.
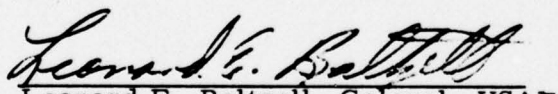
This report has been reviewed by the Information Office (OI) and is releasable to the National Technical Information Service (NTIS). At NTIS, it will be available to the general public, including foreign nations.

This technical report has been reviewed and is approved for publication. Publication of this report does not constitute Air Force approval of the report's findings or conclusions. It is published only for the exchange and stimulation of ideas.

A. G. Fernandez, Lt, USAF
Project Officer

Robert W. Lindemuth, Lt Col
USAF
Chief, Technology Plans Division

FOR THE COMMANDER

Leonard E. Baltzell, Colonel, USAF
Assistant Deputy for Advanced Space
    Programs

REPORT DOCUMENTATION PAGE		READ INSTRUCTIONS BEFORE COMPLETING FORM
1. REPORT NUMBER SAMSO-TR-77-203	2. GOVT ACCESSION NO.	3. RECIPIENT'S CATALOG NUMBER
4. TITLE *(and Subtitle)* MEASURED AND PREDICTED RADIATION-INDUCED CURRENTS IN SEMIRIGID COAXIAL CABLES		5. TYPE OF REPORT & PERIOD COVERED Interim
		6. PERFORMING ORG. REPORT NUMBER TR-0078(3950-04)-1
7. AUTHOR(s) Francis Hai, Paul A. Beemer, Charles E. Wuller (TRW), and David M. Clement (TRW)		8. CONTRACT OR GRANT NUMBER(s) F04701-77-C-0078 DNA 001-77-C-0084
9. PERFORMING ORGANIZATION NAME AND ADDRESS The Aerospace Corporation El Segundo, Calif. 90245		10. PROGRAM ELEMENT, PROJECT, TASK AREA & WORK UNIT NUMBERS
11. CONTROLLING OFFICE NAME AND ADDRESS Space and Missile Systems Organization Air Force Systems Command Los Angeles, Calif. 90009		12. REPORT DATE 11 October 1977
		13. NUMBER OF PAGES 24
14. MONITORING AGENCY NAME & ADDRESS*(if different from Controlling Office)*		15. SECURITY CLASS. *(of this report)* Unclassified
		15a. DECLASSIFICATION/DOWNGRADING SCHEDULE

16. DISTRIBUTION STATEMENT *(of this Report)*

Approved for public release; distribution unlimited.

17. DISTRIBUTION STATEMENT *(of the abstract entered in Block 20, if different from Report)*

19. KEY WORDS *(Continue on reverse side if necessary and identify by block number)*

Satellites
Coaxial Cables
Radiation Response
Radiation Testing

Nuclear Radiation Effects
Plasma Focus
SGEMP

20. ABSTRACT *(Continue on reverse side if necessary and identify by block number)*

Variations in the X-ray-induced response of a number of semirigid coaxial cables are reported. Irradiation spectra were obtained by filtering the radiation from a dense plasma focus device. Semirigid cables of different size, material, and impedance were tested. Minute gaps and conductor flashings were found to be dominant factors affecting cable response. Response predictions provided by the MCCABE computer code closely correlated with the experimental measurements. Design of low-response semirigid cables matching the metal and dielectric electron emission is discussed.

DD FORM 1473 (FACSIMILE)

CONTENTS

FIGURES

TABLE

I. INTRODUCTION

The X-ray-driven currents in several subminiature coaxial cables [1], single braid-shielded wires [2], and braid-shielded multiconductor cables [2, 3] have been reported. The currents induced in these cables ranged from 10^{-14} to 10^{-13} coul/rad(Si)-cm and were found to depend primarily on the separation (gap) between the braid wires and the polymer dielectric. The responses of two spline-dielectric semirigid cables [2] were comparable to those of the braid-shielded coaxial cables because of the large, well-defined gaps between the outer shield and the dielectric.

This paper reports the response values for several solid dielectric semirigid cables. The cables examined differed in size, shield and center conductor materials, and impedance. The variation in response with the spectrum of the incident radiation was also investigated, and the experimental results were compared with the predicted response variations.

II. DPF CABLE TEST ARRANGEMENT

The cable response measurements were taken on the Mk V device in the Dense Plasma Focus (DPF) facility at The Aerospace Corporation. The Mk V DPF device and the experimental arrangement for DPF irradiation of cable samples have been described previously [2]. To observe the low response of the semirigid cable samples (at least a factor of 10 below that of a typical braid-shielded cable), it was necessary to expose 70 to 100 cm of cable, coiling the sample as shown in Fig. 1. The X-ray-induced signals were fed into a low-noise, wide-band amplifier before transmission to the screen room through RG 55 cable carried in a copper conduit. The signals were recorded on Tektronix 7904 and 7844 oscilloscopes, as indicated in Fig. 2.

The test spectra, shown in Fig. 3, were obtained by filtering the initial spectrum (spectrum O) transmitted by the 0.152-cm-thick aluminum window of the sample chamber. The spectrum designations and the corresponding filters are as follows: (1) 0.155-cm aluminum, (2) 0.013-cm copper, (3) 0.025-cm copper, (4) 0.038-cm copper, and (5) 0.053-cm copper. (The copper filters were covered with $\sim$0.025-cm aluminum to eliminate copper fluorescent emission.) The incident radiation was monitored with a 20-μm silicon PIN diode mounted at the center of the cable coil. Variation of the X-ray fluence across the coil was $\lesssim$5% because of the relatively large distance ($\sim$17 cm) between the sample and the radiation source.

For easier comparison with the data reported elsewhere, the cable response data given here has been normalized to the dose in silicon at the external shield surface. The original measurements were, in effect, normalized
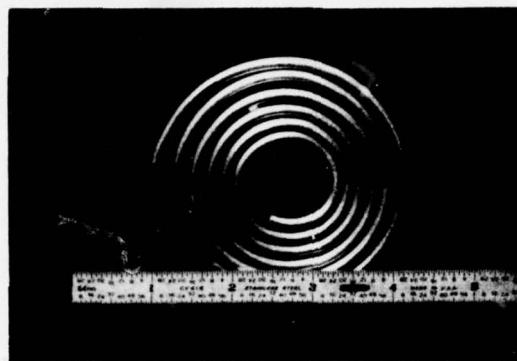
-5-

Fig. 1. Coiled Cable Sample
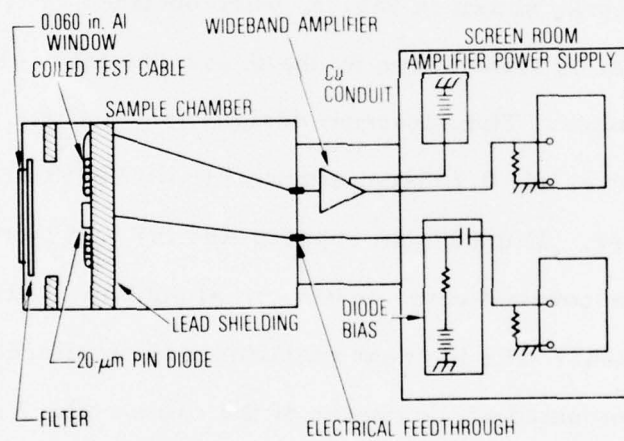
Fig. 2. Schematic of Test Configuration

-6-
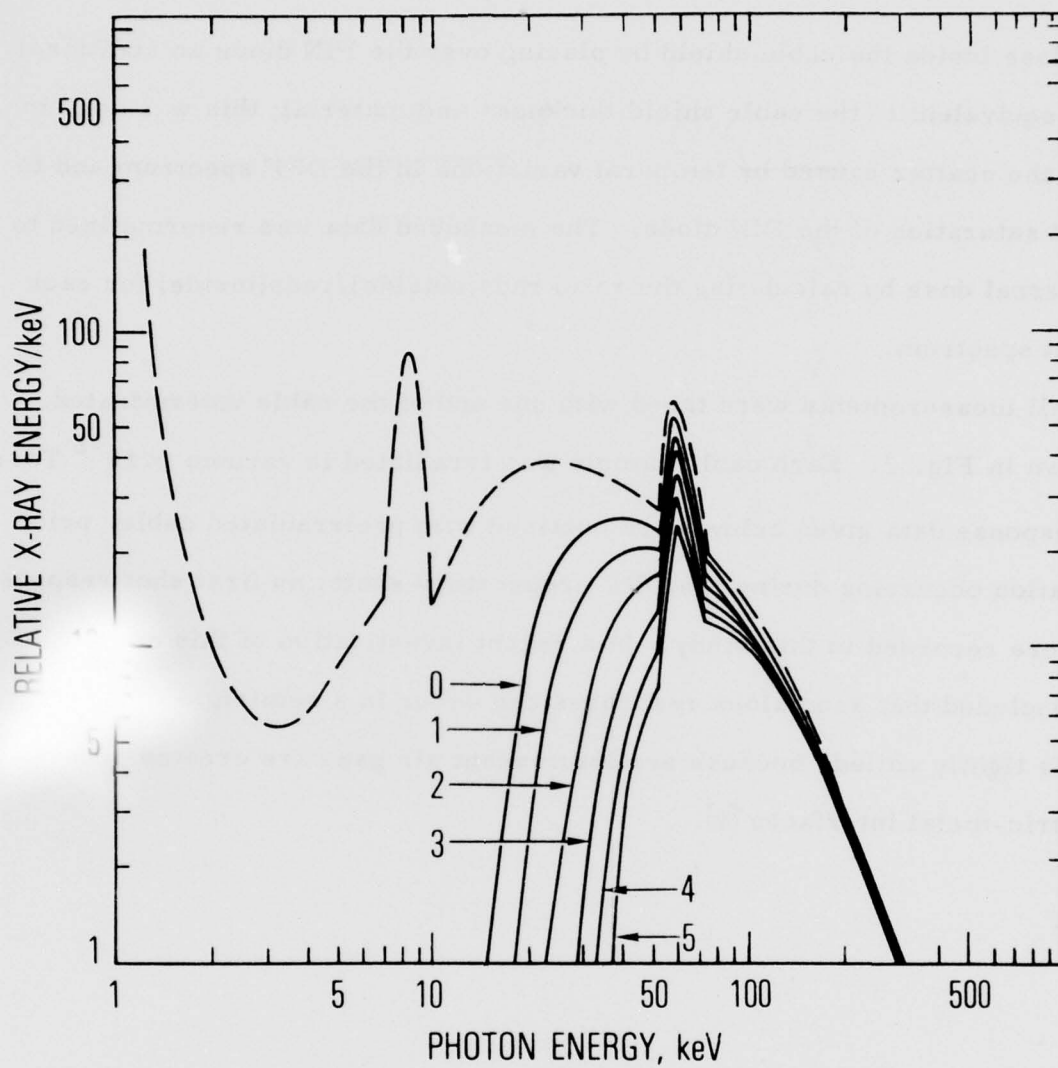
Fig. 3. Dense Plasma Focus Spectra

to the dose inside the cable shield by placing over the PIN diode an additional filter, equivalent to the cable shield thickness and material; this was done to reduce the scatter caused by temporal variations in the DPF spectrum and to prevent saturation of the PIN diode. The measured data was renormalized to the external dose by calculating the ratio rads(outside)/rads(inside) for each incident spectrum.

All measurements were taken with one end of the cable unterminated, as shown in Fig. 2. Each cable sample was irradiated in vacuum ($< 10^{-2}$ Torr). The response data given below were obtained with preirradiated cable, prior irradiation occurring during the DPF preparatory shots; no first shot response data were recorded in this study. In a recent investigation of this effect, it was concluded that anomalous responses can occur in a semirigid cable if the cable is tightly coiled, because semipermanent air gaps are created at the dielectric-metal interfaces [4].

III. SEMIRIGID CABLE DESCRIPTION

A list of the cables tested in this study and a summary of their physical characteristics are given in Table I. All cables are from manufacturers' stock except cables A and B, which are special cables used by the Air Force Weapons Laboratory in electromagnetic pulse (EMP) sensor instrumentation. All cables are of semirigid construction except cable I, which has an inner shield of tape-wrapped copper foil covered with a flexible wire braid; this cable was included in the study because it is functionally equivalent to standard semirigid cables (except that it is flexible) and like them has a minimal dielectric-metal separation. All cable impedances are 50 Ω except that of cable B, which is 100 Ω. All cables have a teflon dielectric except cable F, which has irradiated polyolefin.

Table I. Semirigid Coaxial Cables

Cable Designation	Impedance, Ω	Shield				Center Conductor		Dielectric Material	Manufacturer
		OD, cm	ID, cm	Thickness, cm	Material	Diam, cm	Material		
A	50	0.254	0.203	0.025	Al	0.0620	Al	TFE	Uniform Tubes
B	100	0.254	0.203	0.025	Al	0.0188	Al	TFE	Uniform Tubes
C	50	0.216	0.168	0.024	Al	0.051	Al	TFE	Uniform Tubes
D	50	0.358	0.302	0.028	Al	0.091	Al	TFE	Uniform Tubes
E	50	0.358	0.302	0.028	Al	0.091	SPCW	TFE	Uniform Tubes
F	50	0.546	0.470	0.038	Al	0.129	Cu	IP	Raychem Corp.
G	50	0.216	0.168	0.024	Cu	0.051	SPCW	TFE	Phelps Dodge
H	50	0.358	0.302	0.028	Cu	0.091	SPC	TFE	Phelps Dodge
I	50	0.429	0.368	0.030	F-SPC + S-SPC	0.145	S-SPC	X-TFE	W. L. Gore & Assoc.

Al   aluminum

Cu   copper

SPCW   silver-plated, copper-clad steel

SPC   silver-plated copper

F-   foil

S-   stranded

TFE   tetrafluorethylene (Teflon)

IP   irradiated polyolefin

X-   expanded

Silver layer thickness in SPCW and SPC center conductors $> 1 \times 10^{-4}$ cm.

-10-

IV. MCCABE CODE DESCRIPTION

The MCCABE code was used to obtain the predicted values of the semi-rigid cable responses given in Figs. 4a through 4i. This code was originally developed by TRW to predict differential mode currents in multiconductor cable bundles exposed to X-rays and was subsequently verified by tests conducted in the Simulation Physics SPI-5000 flash X-ray environment [5].

The effect of X-irradiation is to drive electrons from the conductor surfaces and deposit them in the surrounding dielectric materials, thus stimulating the flow of replacement currents. The equivalent circuit which describes electron deposition and replacement currents in an elemental length of N-conductor-plus-shield cable consists of N Norton equivalent drivers and of $N(N+1)/2$ capacitances. A Norton driver is the short-circuit current, i.e., the individual wire current which would flow to ground (assumed to be the shield) through a low impedance load. The capacitances connect all pairs of conducting surfaces. Such an equivalent circuit is valid under the following conditions:

1.   Propagation is TEM, i.e., the electric field is derivable from a scalar potential.

2.   Propagation is lossless (resistivity, polarization losses, and radiation-induced dielectric conductivity must be negligible).

3.   Electron transport is independent of local fields, i.e., the collisional stopping power controls electron deposition.

The MCCABE code calculates Norton drivers and capacitances for a cable geometry in which all conductor surfaces are cylindrical. Electron
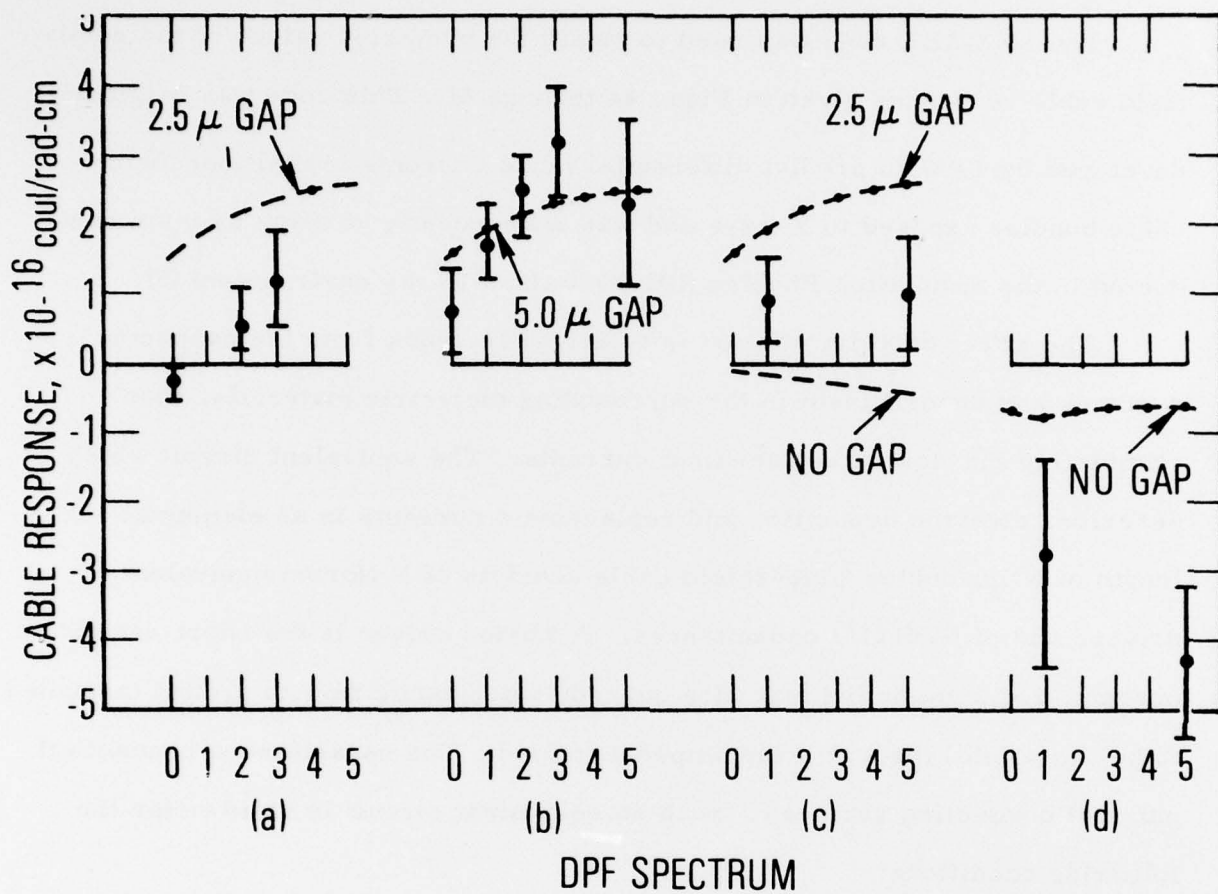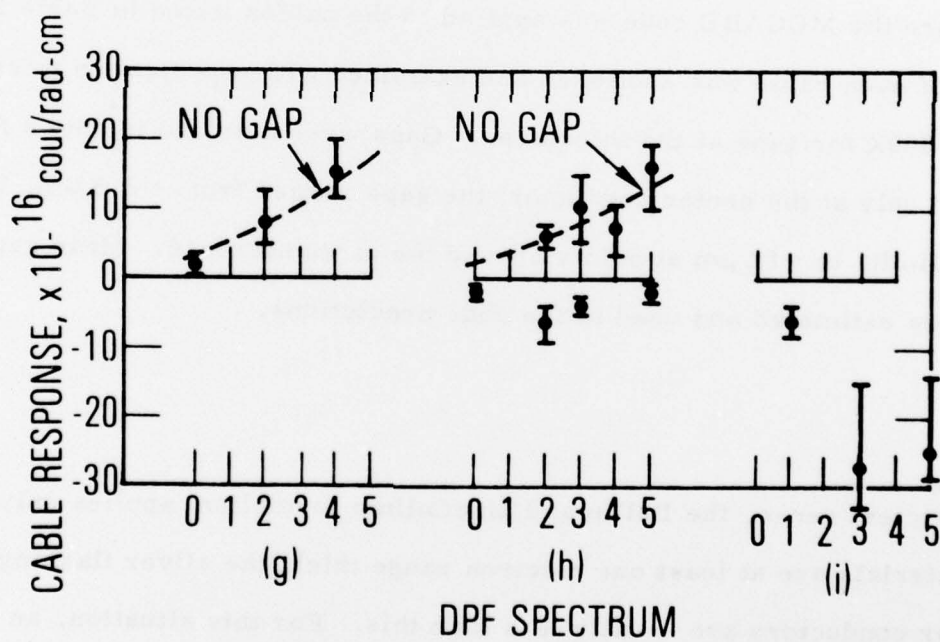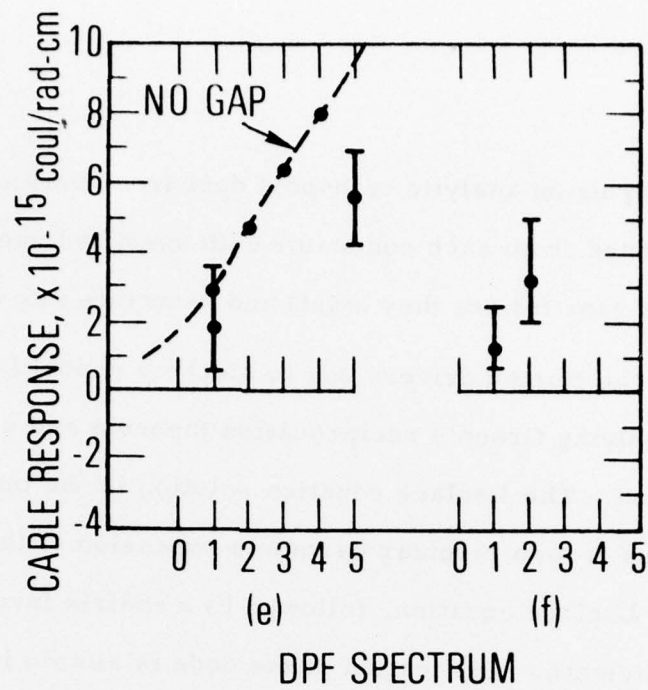
-11-

Fig. 4. Cable Response Data

Fig. 4. Cable Response Data (Continued)

9

deposition is found by using analytic transport data from Dellin and MacCallum [6]. Electrons, emitted from each conductor with specified energy and angular distributions, cross gaps (where they exist) and penetrate into dielectrics.

The contribution to the Norton drivers due to electron deposition at a given point is found by applying Green's reciprocation theorem and using a solution of Laplace's equation. The Laplace equation solution in the multiconductor geometry is obtained from a circular harmonic expansion of the integral equation solution to the Laplace equation, followed by a matrix inversion to obtain the expansion coefficients. Application of the code is simple in the case of a coaxi   cable, where $N = 1$.[†]

    ore the MCCABE code was applied to the cables listed in Table I, a sa   of each cable was sectioned and examined with a projection micro-scope   t 1000X for gaps at the interfaces. Gaps were detected in only a few cables and only at the center conductor; the gaps ranged from ~ 2.5 μm, the detection limit, to ~ 12 μm at points around the circumference. Mean gap values were estimated and used in the code predictions.

[†]In the strictest sense, the Dellin and MacCallum formalism applies only when cable materials are at least one electron range thick; the silver flashings on the center conductors are usually less than this. For this situation, an algorithm based on an approximate solution to the Spencer-Lewis transport equation was developed; details are given in the Appendix.

V. RESULTS AND DISCUSSION

The radiation responses of the cables are given in Figs. 4a through 4i as a function of the incident X-ray spectrum. The heavy points represent the average values from a number of shots; the bars indicate the range of the measured values. (The scatter in the data is the result of temporal variations in the DPF spectrum; measurement uncertainties are ~10%.) Fig. 4 also includes the responses predicted by the MCCABE code (indicated by the dashed lines on the charts) and the assumed average gap sizes. No predictions were made for cables F or I.

All cable theories predict a negative response for a gapless semirigid cable with identical conductor materials. In reality, a truly gapless cable cannot be made; since the penetration range of a 30-keV electron in solid teflon is ~4 μm, a gap only a few microns wide will dominate the electron transport and hence the induced response.

This effect is clearly illustrated by the positive responses of cables A, B, and C. These cables were made by sleeving an aluminum wire with an appropriate teflon tube, sliding the insulated wire into a shield of aluminum, and then collapsing the tubing onto the dielectric by drawing the cable through a sizing die. Because of the low tensile strength of the aluminum center conductors, the swaging forces used were much less than those used in the manufacture of cables D and E, which have stronger center conductors. (Cables A through E were made by the same manufacturer.)

The response of cable A was somewhat less than that predicted from the gap measurements; considering the small negative response at the softest spectrum, this was probably caused by residual gas trapped within the gaps. The predicted response of cable B, based on the better-defined gaps in that cable, was in excellent agreement with the data. Cable C, although it had no detectable gaps, gave a positive response which lay between the predicted values based on no gap and a 2.5-μm (detection limit) gap. The response of cable D was negative, as theory would predict. However, the response was several times larger than that predicted for a gapless cable, which may indicate the presence of significant gaps at the outer conductor interface. Although no gaps were visible in an uncoiled sample, such gaps would probably have been created when the large-diameter cable was bent in a short-radius coil.

The responses of cables E, F, and G were all positive, consistent with the high-Z center conductors of these cables. The MCCABE predictions for cables E and G, based on the nominal 2.5-μm thickness of the silver plating, are in good agreement with the data; predictions assuming that the center conductor was pure silver were ~3× larger.

Cable H, the 141 copper semirigid cable, gave a bipolar response at all test spectra, with an initial negative response that was later swallowed by a positive pulse. From the signal polarity, it seems reasonable to conclude that this was caused by the presence of air-filled gaps between the dielectric and the outer jacket. Since no gaps were detected in an unbent sample, it would again appear that the gaps were formed when the cable was coiled,

presumably because the teflon was pulled away from the outside surface. Un-like the case of the semirigid cable tested in Ref. 2, however, the gaps showed no sign of pumping out, even after 10 days at $p < 10 \mu$; nor did the teflon relax after "_____" for several hours at 100°C and for 1 hour at 125°C.

Finally, cable I gave the typical negative response of a gapless cable. The tape-wrapped expanded teflon dielectric is tightly pressed onto the center conductor, and the foil outer conductor is tightly wrapped onto the dielectric; because of the cable's flexibility, no gaps were created when the cable was coiled. The response was ~2× larger than that of an equivalent copper cable because of the enhanced emission from the silver-plated surfaces.

VI. DIELECTRIC-METAL COMBINATIONS IN SEMIRIGID CABLES

In all readily available semirigid coaxial cables, the conductors are high-Z metals and the dielectrics are low-Z polymers. For such cables, electron emission from the metal into the dielectric is always much larger than that in the other direction. (The MCCABE code neglects electron emission from the dielectric.) Even in the aluminum-teflon cables, emission from teflon is only $\sim 30\%$ of that from aluminum for DPF spectra. Because of this large unidirectional electron flux, gaps occurring at either the shield or center conductor interface greatly affect the response of the cable.

The net electron flux can be reduced by selecting a metal and a polymer with matched electron emissivities. Simple analysis indicates that emission from Matex, an aluminum-beryllium alloy, would be well matched to that from teflon; however, the availability and the physical properties of Matex do not favor fabrication of such a cable. Analysis indicates that emission from Kel-F (C_2ClF_3) would be well matched to that of aluminum. Measurements show that photoemission from Kel-F is $\sim 83\%$ of that from aluminum, while Halar, a copolymer of Kel-F and polyethylene, has a relative emissivity of $\sim 70\%$. Semirigid cables with either of these dielectrics should have lower X-ray responses, since the net driving current at each interface will be reduced.

VII. CONCLUSION

The X-ray responses of the semirigid cables studied were determined primarily by gaps produced during fabrication or handling, high-Z metal flashings on the center conductor, and differences in emission between the shield and the center conductor. The MCCABE code, capable of incorporating gap widths and flashing thicknesses into its analysis of semirigid cable response, can closely predict the response of these cables. Semirigid cables with X-ray responses lower than those observed in this study can be obtained through careful selection of conductor and dielectric and improved fabrication techniques.

REFERENCES

[1]   M. J. Bernstein, "Radiation Induced Currents in Subminiature Coaxial Cables," IEEE Trans. on Nucl. Sci. NS-20, 6, pp. 58-63 (December 1973).

[2]   R. L. Fitzwilson, M. J. Bernstein, and T. E. Alston, "Radiation Induced Currents in Shielded Multiconductor and Semirigid Cables," IEEE Trans. on Nucl. Sci. NS-21, 6, pp. 276-283 (December 1974).

[3]   E. P. Chivington, L. E. Shaw, and T. E. Alston, "Radiation Induced Common Mode and Individual Wire Current Response of Shielded Twisted Pair Cables," IEEE Trans. on Nucl. Sci. NS-23, 6, pp. 1952-1957 (December 1976).

[4]   D. M. Clement, L. C. Nielsen, and C. E. Wuller, "Stored Charge Release in Cables in Low Fluence X-Ray Environments," IEEE Conference on Nuclear and Space Radiation Effects, paper F-13, Williamsburg, Virginia, July 1977.

[5]   D. M. Clement, C. E. Wuller, and E. P. Chivington, "Multiconductor Cable Response in X-Ray Environments," IEEE Trans. on Nucl. Sci. NS-23, 6, pp. 1946-1951 (December 1976).

[6]   T. A. Dellin and C. J. MacCallum, "Photo-Compton Currents Emitted From a Surface," J. Appl. Phys. 46, p. 2924 (1975).

APPENDIX

AN APPROXIMATE TREATMENT OF THE EFFECTS OF FINITE
FLASHING THICKNESS ON ELECTRON TRANSPORT

The objective here is to develop an approximate expression for the emission efficiencies from a conductor when the flashing thickness is less than an electron range thick. The starting point is the one-dimensional Spencer-Lewis transport equation, with a monochromatic source of electrons and without the collision term

$$\left(\cos\theta \frac{d}{dz} + \frac{d}{ds}\right) f = \delta(s) \, FN\sigma \tag{1}$$

where $f(\vec{r}, \vec{\Omega}, s)$ is the number of electrons per unit solid angle, time, residual path length, and volume and where the path length s is defined as

$$s = \rho \int_E^{E_{max}} dE \left|\frac{dE}{dx}\right|^{-1} = \rho\left[\bar{r}(E_{max}) - \bar{r}(E)\right] \tag{2}$$

where ρ is the density, dE/dx the stopping power, and $\bar{r}$ the range in g/cm^2 (cf. Fig. A-1). In addition, F is the monochromatic incident number flux of photons of energy E; N is the atomic number density; and σ is the atomic differential cross section for photon-electron scattering. The right-hand side of (1) represents the source term in the equation (i.e., the number of

electrons created per unit time, solid angle, and volume), and E_{max} is the maximum electron energy (E minus the binding energy).

We will make the following assumptions:

1. N and ρ are constants, obtained by averaging over the conductor materials in question.

2. F, the photon flux, is independent of $\vec{r}$ over the region of interest.

3. The electron ranges in both conductors are the same.

4. The omission of the collision term in the equation will be taken into account by the use of bulk emission efficiencies of Dellin-MacCallum rather than the "bare" efficiencies described below.
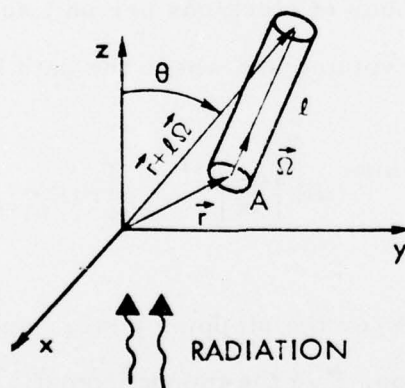
Fig. A-1. Definition of the Distribution Function $f(\vec{r}, \Omega, s)$, Where $f(d\Omega)(ds)A\ell$ Is the Number Transported Into the Volume per Second

We solve (1) for the case of three slabs of material (Fig. A-2). We are interested first in the case of $\cos \theta > 0$, i.e., forward going electrons. The boundary conditions (cf. Fig. A-2) are:

$$f = 0 \text{ at } z = 0.$$

f is continuous at the interfaces.[§]

The first condition merely expresses the fact that no forward electrons are created at the left of the first slab. The formal solution for the distribution function for the ith slab is
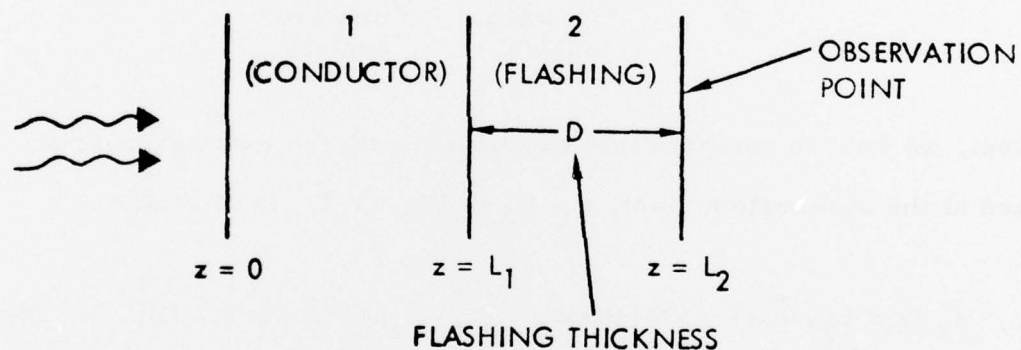

Fig. A-2. Slab Model for Defining Boundary Conditions for Forward-Going Electrons

---

[§]If we allowed for different densities of material, the second boundary condition would be $\rho_i^{-1} f_i = \rho_{i+1}^{-1} f_{i+1}$.

-27-

$$f_i = FN \left\{ H(s) \, \sigma_i - \sum_{j=1}^{i} \left[\sigma_{i-j+1} - (1 - \delta_{ij}) \, \sigma_{i-j} \right] \cdot \right.$$

$$\left. \cdot \left[s \cos \theta - (z - L_{i-1}) - (1 - \delta_{j1}) \sum_{k=i+1-j}^{i-1} (L_i - L_{i-1}) \right] \right\} \tag{3}$$

where H is the step function.

For an infinite homogeneous media, $f = H(s) \, FN\sigma$, and the number of electrons/time $\cdot$ area moving forward per unit photon flux (i.e., the yield) is

$$e^{(\infty)} = \frac{1}{F} \int_{o}^{\overline{r}/\rho} ds \int_{\substack{\text{forward} \\ \text{angles}}} d\Omega f \; = \frac{N\overline{r}}{\rho} \int_{\substack{\text{forward} \\ \text{angles}}} d\Omega \sigma \tag{4}$$

Next, we want to compare this expression with the exact expression generated at the observation point, $z = L_2$ in Fig. A-2. In this case

$$f_2 (z = L_2, \vec{\Omega}, s) = FN \left[H(s)\sigma_2 + (\sigma_1 - \sigma_2) \, H (s \cos \theta - D) \right] \tag{5}$$

If we approximate $\cos \theta$ by unity in this expression, we obtain a simple expression for the electron photon yield, in terms of that for the infinite homogeneous media associated with slabs 1 and 2

$$e = \frac{1}{F} \int^{\overline{r}/\rho} ds \int_{\substack{\text{forward} \\ \text{angles}}} d\Omega \quad f_2 (z = L_2, \vec{\Omega}, s)$$

$$= e_2^{(\infty)} + \left(e_1^{(\infty)} - e_2^{(\infty)} \right) \left(1 - \frac{\rho D}{\overline{r}} \right) H\, (\overline{r} - \rho D) \tag{6}$$

Here, $D = L_2 - L_1$, the flashing thickness.

The significance of the expression is as follows: if the flashing thickness D is greater than an electron range, $e = e_2^{(\infty)}$, i.e., the flashing is the emitter. If D is less than an electron range

$$e = e_1^{(\infty)} + \left(e_1^{(\infty)} - e_2^{(\infty)} \right) \frac{\rho D}{\overline{r}}, \quad \rho D < \overline{r} \tag{7}$$

Then the yield $e_1^{(\infty)}$ (i.e., of the material without the flashing) is "corrected" by an amount determined by the difference in bulk efficiencies of both materials, as well as the flashing thickness and range.

Although (7) was derived from the Spencer-Lewis equation <u>without</u> the appropriate collision term, in (6) we use the Dellin-MacCallum yields that have these terms in them, and our results to some extent have been correctly renormalized.

A similar expression results for the backward emission.

THE IVAN A. GETTING LABORATORIES

The Laboratory Operations of The Aerospace Corporation is conducting experimental and theoretical investigations necessary for the evaluation and application of scientific advances to new military concepts and systems. Versatility and flexibility have been developed to a high degree by the laboratory personnel in dealing with the many problems encountered in the nation's rapidly developing space and missile systems. Expertise in the latest scientific developments is vital to the accomplishment of tasks related to these problems. The laboratories that contribute to this research are:

Aerophysics Laboratory: Launch and reentry aerodynamics, heat transfer, reentry physics, chemical kinetics, structural mechanics, flight dynamics, atmospheric pollution, and high-power gas lasers.

Chemistry and Physics Laboratory: Atmospheric reactions and atmospheric optics, chemical reactions in polluted atmospheres, chemical reactions of excited species in rocket plumes, chemical thermodynamics, plasma and laser-induced reactions, laser chemistry, propulsion chemistry, space vacuum and radiation effects on materials, lubrication and surface phenomena, photosensitive materials and sensors, high precision laser ranging, and the application of physics and chemistry to problems of law enforcement and biomedicine.

Electronics Research Laboratory: Electromagnetic theory, devices, and propagation phenomena, including plasma electromagnetics; quantum electronics, lasers, and electro-optics; communication sciences, applied electronics, semiconducting, superconducting, and crystal device physics, optical and acoustical imaging; atmospheric pollution; millimeter wave and far-infrared technology.

Materials Sciences Laboratory: Development of new materials; metal matrix composites and new forms of carbon; test and evaluation of graphite and ceramics in reentry; spacecraft materials and electronic components in nuclear weapons environment; application of fracture mechanics to stress corrosion and fatigue-induced fractures in structural metals.

Space Sciences Laboratory: Atmospheric and ionospheric physics, radiation from the atmosphere, density and composition of the atmosphere, aurorae and airglow; magnetospheric physics, cosmic rays, generation and propagation of plasma waves in the magnetosphere; solar physics, studies of solar magnetic fields; space astronomy, x-ray astronomy; the effects of nuclear explosions, magnetic storms, and solar activity on the earth's atmosphere, ionosphere, and magnetosphere; the effects of optical, electromagnetic, and particulate radiations in space on space systems.

THE AEROSPACE CORPORATION
El Segundo, California

. . .